

We are IntechOpen, the world's leading publisher of Open Access books Built by scientists, for scientists

4,800

Open access books available

122,000

International authors and editors

135M

Downloads

Our authors are among the

154

Countries delivered to

TOP 1%

most cited scientists

12.2%

Contributors from top 500 universities



WEB OF SCIENCE™

Selection of our books indexed in the Book Citation Index
in Web of Science™ Core Collection (BKCI)

Interested in publishing with us?
Contact book.department@intechopen.com

Numbers displayed above are based on latest data collected.
For more information visit www.intechopen.com



Electron Microscopy and Microanalysis of the Fiber, Matrix and Fiber/Matrix Interface in SiC Based Ceramic Composite Material for Use in a Fusion Reactor Application

Tea Toplisek¹, Goran Drazic¹, Vilibald Bukosek²,
Sasa Novak¹ and Spomenka Kobe¹

¹*Institute Jozef Stefan, Department for Nanostructured Materials*

²*Faculty of Natural Science and Engineering
Slovenia*

1. Introduction

Composite materials are engineered materials made from two or more constituent materials. They have significantly different physical or chemical properties which remain separate and distinct on a macroscopic level within the finished structure. The advantage of composite material is that they exhibit the best qualities of their components or constituents and often some qualities that neither constituent possesses. The properties that can be improved by forming a composite material are strength, stiffness, corrosion resistance, wear resistance, weight, thermal insulation, thermal conductivity, etc. Composite materials can be classified and characterized into four commonly accepted types; (1) fibrous composite materials that consist of fibers in a matrix, (2) laminated composite materials that consist of layers of various materials, (3) particulate composite materials that are composed of particles in a matrix and (4) the combination of some or all the first three types (Jones, 1999). According to the matrix phase the composites are divided into three groups; (1) metal matrix composites (MMCs), (2) polymer matrix composites (PMCs) and (3) ceramic matrix composites (CMCs). Ceramic materials in general have very attractive properties e.g.: high strength and high stiffness at very high temperatures, chemical inertness and low density. In the presence of flaws (surface or internal) they are prone to catastrophic failures. Ceramic materials can be toughened by incorporating fibers and thus exploit the attractive high-temperature strength and environmental resistance of ceramic materials without risking a catastrophic failure (Chawla, 1987). According to the basics written above, a monolithic silicone carbide (SiC) was used as a matrix phase, which has been recognized as one of the most promising structural materials for many thermo-mechanical applications because of its excellent high-temperature strength and modulus, good oxidation resistance, high hardness, low specific weight and low density (Xin-Bo & Hui, 2005; Xin-Bo et al., 2000; She et al., 1999). The problem with monolithic SiC is its low thermal shock resistance, which leads to cracking and catastrophic failure of the material. Thermal shock resistance and crack propagation can

be improved by introducing a reinforcement phase, continuous SiC fibers, into the monolithic SiC matrix to produce a SiC_f/SiC composite material (Kowbel et al., 1995). This kind of composite materials is being considered for a future fusion reactor because of its low induced radioactivity after neutron irradiation, non-catastrophic failure mode, specific thermal conductivity and low porosity (Zhang et al., 1998; Taguchi et al., 2005). It is known that the properties of the fiber/matrix interface play an important role in determining the mechanical and physical properties of ceramic matrix composites (CMCs). It can be defined as a bonding surface where a discontinuity of some kind occurs. In general it is a bidimensional region through which material parameters, such as concentration of an element, crystal structure, atomic registry, elastic modulus, density, and coefficient of thermal expansion, change from one side to another. It is important to be able to control the degree of bonding between the matrix and the reinforcement. The pure mechanical bonding usually is not enough but it is efficient in load transfer when the applied force is parallel to the interface. The chemical bonding is also important and can be divided into two types; dissolution and wettability bonding, where surface should be appropriately treated to remove any impurities; and reaction bonding where a transport of atoms occurs from one or both of the components to the reaction site, the interface (Chawla, 1987). In general, if the fiber/matrix interface is weak, the composite has low strength and stiffness, but a high resistance to fracture. In the case of a strong interface, which allows a crack to propagate straight through the fibers, the strength and stiffness of the composite are high, but the composite itself is brittle (Xin-Bo & Hui, 2005; Xin-Bo et al., 2000; Bertrand et al., 2001; Nuriel et al., 2005). However, the composite's brittleness remains a problem. This can be improved by adding a thin film of compliant material, called the "interphase", between the fiber and the brittle matrix, which has three main functions: protection of the fibers, load transfer between the fiber and the matrix and control of the crack deflection at the interface (Zhang et al., 1998; Jacques et al., 2000; Bertrand et al., 2000). The most commonly used interphase materials for SiC_f/SiC composites are pyrolytic carbon (PyC), boron nitride (BN) and, recently, a multilayer of (PyC/SiC). All these materials have their advantages and disadvantages. PyC has low oxidation resistance; BN is not suitable for fusion applications because the nitrogen transmutes into ¹⁴C, which has a very long half-life as a β emitter after the neutron irradiation.

The processing of SiC_f/SiC is a complex, multi-stage process. Common processing techniques for the production of SiC_f/SiC composites include chemical vapor infiltration (CVI), polymer impregnation and pyrolysis (PIP), molten silicon infiltration (MI), reaction sintering (RS) and the nano-infiltrated transient eutectoid (NITE) process (Katoh et al., 2002). In this paper we present a microstructural and micro-indentation study of a material, fabricated by a novel method for preparing SiC_f/SiC composite materials for fusion-reactor applications. The method consists of the adapted dip coating and infiltration of the SiC-fibers with a water suspension of SiC-particles and sintering additives. In order to study the crack deflection, introduced by the Vickers indenter, we deposited various layers (diamond-like carbon (DLC), CrC, CrN and WC) on the fibers' surface using physical vapor deposition. A comparison between the uncoated and coated fibers was made.

The microstructures of the SiC_f/SiC composite materials with different interphases between the fibers and the brittle matrix were examined using conventional transmission electron microscopy (TEM) and high-resolution (HR) TEM.

Specimen preparation methods for ceramic fibers are often unsatisfactory. We tried to optimize and develop different preparation techniques which have an important role in study of these materials.

The fracture surfaces of the samples were observed using scanning electron microscopy (SEM). Z-contrast imaging (STEM/HAADF) and different techniques of electron diffraction were applied for the phase identification. The chemical composition of the individual phases was determined using XEDS.

2. Materials and Methods

The starting material was commercially available 0.5 μm SiC powder BF-12 (HC Starck, Goslar, Germany), Nicalon and Hi-Nicalon Type S fibers (COI Ceramics, San Diego, CA), Tyranno SA fibers (UBE Industries LTD., Düsseldorf, Germany), aluminium dihydrogen phosphate, Bindal A (TKI Hrastnik, Slovenia), anionic surface active agent, sodium dioctylsulfosuccinate, SDOSS and polymer Starfire (Starfire systems, Malta, NY).

Among several known methods for the preparation of the SiC_f/SiC composite material, which are described elsewhere (Drazic et al., 2005; Novak et al., 2006; Novak et al., 2010), we used infiltration with micro particles suspension. The process begins with immersion of the fibers into a water suspension made from micro-sized particles and a sintering additive based on the Al-Si-P-O system, dip-coating and drainage. All samples were sintered at 1300 °C in pure argon. Because of the hydrophobic nature of the fibers we impregnated them with anionic surface active agent. It consists of liophobic and liophilic groups, which arrange on the substrate surface in a way to increase its wettability with our water suspension.

Using reactive sputtering the fibers were coated with a thin layer of interphase material (CrC, WC and diamond like carbon - DLC) with relevant chemical composition in terms of neutron activation. The coatings were sputtered with a Sputron (Balzers AG, Liechtenstein). The thickness of the interphase layer was varied between a few and 500 nm, depending on the experimental conditions and geometry of the fibers (overlapping) during the deposition. The nanohardness of the fibers and the matrix was measured using Vickers indenter on the Fischerscope instrument H100C (Helmut Fischer, Germany), which records indentation depth and load. The load we used was in both cases 10 mN. On the other hand, a Vickers microhardness tester (MVK-H2 Hardness tester, Mitutoyo, Japan) was used in order to observe the cracks in the matrix and its deviation from the primary direction. A maximum load of 1 N was applied in order to initiate the cracks.

The mechanical properties of the coated and uncoated fibers were also measured on dynamometer Instron 5567 (Instron, Great Britain). The fiber was put between two clamps and extended till breaking. With special program we can follow internal changes in material structure during testing. This program also allows later interpretation of all values that were measured.

For observing the samples' surface, morphology, topography and the particles size we used scanning electron microscope, JEOL JSM-5800. The working voltage was 20 keV. The energy-dispersive X-ray spectrometer (Link ISIS 300, Oxford Instruments) was used for determining the chemical composition.

The fibers' topography was also observed with atomic force microscopy (VEECO Dimension 3100) before and after the coating.

Ceramic fibers are key components in a number of technologically important applications, such as reinforcements in structural ceramic matrix composites. Application of transmission electron microscopy is often required for characterization of such fibers. Preparation of electron transparent sections of thin ceramic fibers is a challenging task often limits the use of TEM studies on such fibers (Mogilevsky, 2001). A special paragraph is dedicated to the TEM specimen preparation techniques. The structure and chemical composition of the materials on micrometer, nanometer or even atomic level were set and characterized with transmission electron microscope, JEOL 2010 F FEG-STEM and JEOL 2100 and a Link ISIS 300M XEDS analysis.

3. TEM Specimen Preparation Techniques

Different techniques were used for TEM specimen preparation because of the variety of the samples. The basic goal of the specimen preparation is to get a thin area (thickness from 10 to 50 nm) in the material to be transparent for the electrons with high energy (from 100 keV to 200 keV). It is desired that this area is as big as possible, that it has uniform thickness and should not cause artifacts in a way of changing the chemical structure or the structure itself (amorphization or crystallization). It is also important that during the preparation we do not put the impurities on the samples which can cause a contamination of the sample in the microscope (Gec & Ceh, 2006).

The conventional technique which is mechanical thinning, dimpling and ion-milling was used for the bulk material. This method is not suitable for observing the SiC fibers because the fibers are much stiffer than the epoxy in which the fibers are embedded during the preparation. Problems also occur during ion-milling; the fibers are either not transparent for the electrons or they are pulled out of the high-temperature epoxy. So we looked for the alternative methods. Some of the methods we used are described later on.

The first method (Figure 1) is very simple and fast. The fibers are prepared by gluing them parallel on a TEM grid or a ring, finally cured on a hot plate and ion-milled (Bal-Tec RES 010) till the perforation.

The second method (Figure 2) combines a technique for preparing fiber/epoxy assemblies with mechanical polishing to a thickness of less than 5 μm , thus minimizing the time of ion milling (Mogilevsky, 2001). Fibers are put between two 500 μm glasses coated with high-temperature epoxy, clamped with a pair of Teflon plates to squeeze out excessive epoxy and finally cured on a hot plate. This sandwich structure was first thinned on diamond lapping films (Allied) of different gradation, using a Tripod Polisher (Allied) till approximately one half of the fibers' diameter. Then a TEM grid was glued on the polished surface to strengthen the specimen. This grid was also used for thickness measurements during the polishing. It is important that no air bubbles are trapped between the grid and polished side of the specimen. The thinning process is continued on the other side of the specimen to the final thickness of less than 5 μm . The thinned sample was milled in ion miller at 4 keV with incident angle of 10° until a perforation was observed. This method requires a long preparation time, frequent observations under the optical microscope to ensure parallel thinning and accuracy. The method can be extended to other types of materials, such as fiber-reinforced ceramic composites.

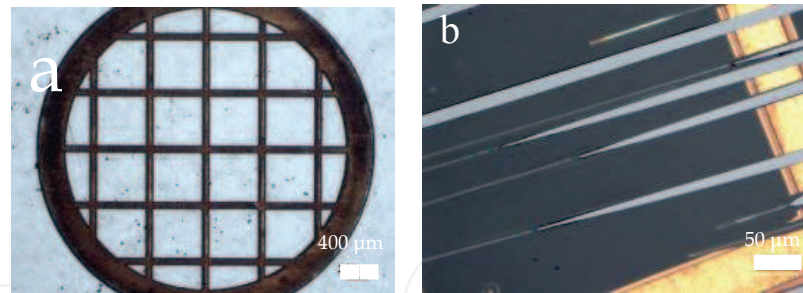


Fig. 1. Optical micrographs: (a) TEM grid on which the fibers were glued parallel and (b) interferences in Tyranno SA SiC fibers after ion-milling.

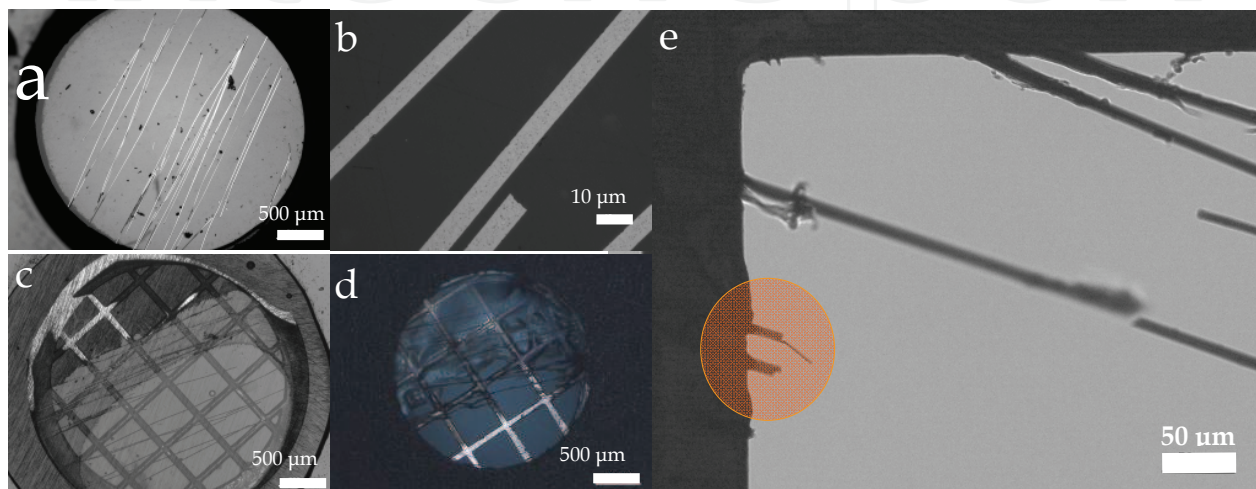


Fig. 2. Optical micrographs of the Tyranno SA SiC fibers using tripod polishing method: (a) specimen polished on one side through approximately one half of the fiber diameter; (b) same as in (a) but at higher magnification; (c) specimen mounted on a supporting grid, turned over and polished to the final thickness; (d) specimen after ion-milling; (e) same as in (d) but at higher magnification. The marked circle is transparent enough for observing with transmission electron microscope.

For observing the coatings on the fiber surface, the cross-section method was used. It is important to have a high ratio between the fibers and epoxy. The fibers were cut on short segments and put parallel into the groove made in silicon plate. To get a sandwich structure another silicon plate was put on it and clamped between two Teflon plates to squeeze out excessive epoxy, followed by curing on a hot plate. Then the sandwich structure was put into a brass ring with blind tracks to strengthen the sample. A conventional technique was used further on. Figure 3 show optical micrographs of Nicalon SiC fibers coated with a thin layer and prepared as a cross-section by conventional method including mechanical thinning, dimpling and ion-milling. Figure 3a shows optical micrograph of coated fibers in the groove between Si plates after dimpling. The thickness in the center of the specimen is 16 μm . After mechanical thinning, the quality of the specimen is improved with polishing to eliminate all the imperfections in the sample. This sample is ready for ion-milling. Figure 3b shows the same sample as in Figure 3a but after ion-milling. The sample was bombarded with Argon ions till the perforation. Because of the difference in hardness, we can see that epoxy resin starts to ion-mill much faster and quicker than the SiC fibers.

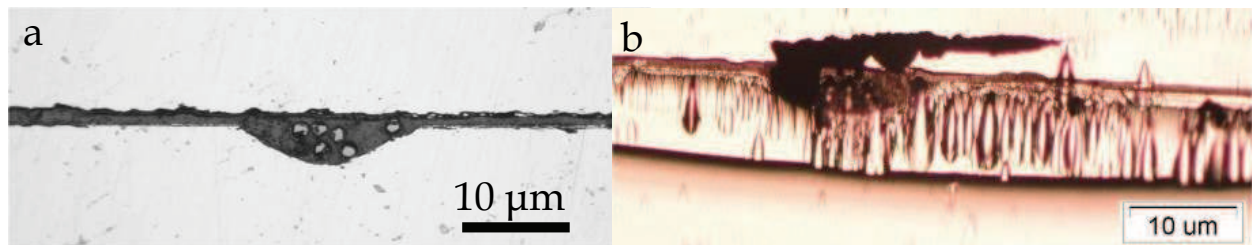


Fig. 3. Optical micrographs of the Nicalon SiC fibers coated with a thin layer and prepared as cross-section by conventional method: (a) after dimpling; (b) after ion-milling.

The SiC_f/SiC samples were prepared by conventional method (Figure 4a) and a wedge-polishing method (Figure 4b) which allows very accurately controlled thinning. In a conventional method, thin foils were cut on a wire saw from the composites, perpendicular to the fiber axis. After mechanical thinning to a thickness of approximately 80-100 μm the samples were polished to a final thickness of 20 μm , by dimpling. Ion-milling was used as a final step to get a perforation of the samples. TEM investigation revealed more or less complete erosion of the matrix during the preparation process. The mechanical thinning with a wedge-polishing method was performed on diamond lapping films at a very small wedge angle of 1° . This method is far superior than the conventional ion-milling. It is suitable for any multiphase specimens with large hardness differences.

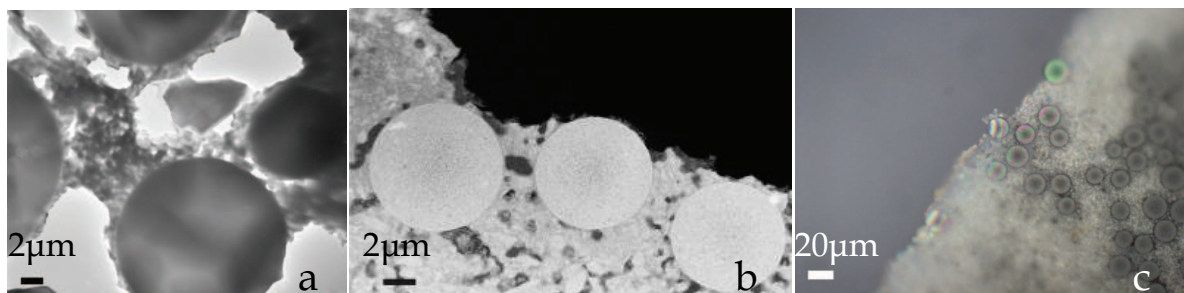


Fig. 4. TEM and optical micrographs of SiC_f/SiC composite material: (a) SiC_f/SiC after ion-milling where erosion of the matrix is visible; (b) HAADF-STEM micrograph of SiC_f/SiC prepared by tripod polishing; (c) Optical micrograph of tripod polished specimen prepared as a cross-section where interference fringes at the edge of the specimen are visible.

4. Results and Discussion

4.1 The Microstructure of the SiC fibers

As mentioned above we used different SiC fibers; Nicalon, Hi-Nicalon S and Tyranno SA. In this paragraph the microstructure, the topography and the chemical composition will be discussed for all three SiC fibers.

Figure 5a shows SEM micrograph of the Nicalon SiC fiber with a diameter of 15 μm . Its surface is smooth and without any visible defects. The fibers are consisted of Silicon, Carbon and Oxygen in a determined ratio. A detailed TEM analysis revealed that at room temperature these fibers consist of amorphous matrix phase (Figure 5b) with a small amount of $\beta\text{-SiC}$ nanocrystallites, 1-3 nm in size. The SAED pattern (Figure 5c) shows diffused rings which can be indexed as cubic SiC. In the inset of SAED pattern (Figure 5c) simulated

pattern is displayed. For calculations EMS program code was used (Stadelmann, 1987) and particle size of 1 nm. The average roughness of the amorphous Nicalon SiC fibers was measured on AFM (Figure 5d) and was around 2 nm.

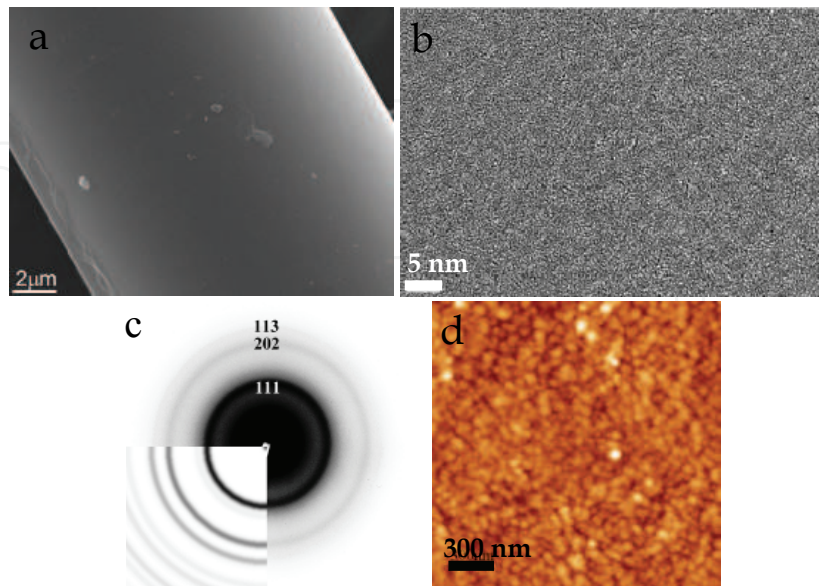


Fig. 5. Nicalon SiC fiber: (a) SEM micrograph; (b) HR-TEM micrograph; (c) Diffraction pattern; (d) AFM micrograph.

Contrary to the Nicalon SiC fibers, the Hi-Nicalon S SiC fibers consist of two clearly defined phases (Figure 6b); crystalline phase in the inner part of the fiber and amorphous phase in the outer part of the fibers. The crystalline phase consists of SiC crystallites, 5 to 20 nm in size; while the amorphous phase was determined as pyrolytic carbon in a lamellar microstructure. From the SEM micrograph (Figure 6a) we can see that the fiber has a diameter of 12 μm , the surface morphology is similar to the Nicalon SiC fibers.

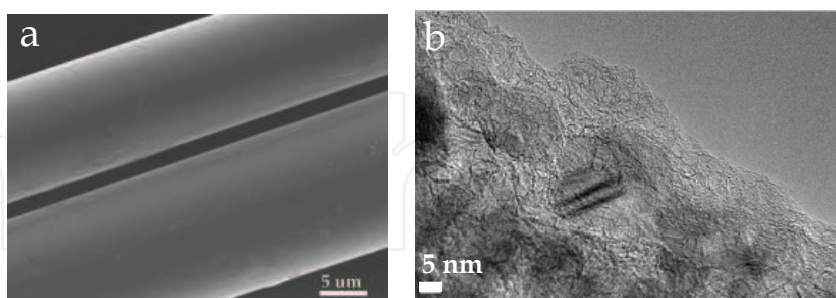


Fig. 6. Hi Nicalon S SiC fiber: (a) SEM micrograph; (b) TEM micrograph.

The newest SiC fibers are Tyranno SA SiC fibers with a diameter of 7 μm . The surface is much rougher than the surface of the Nicalon SiC fibers but also without any imperfections (Figure 7a). The roughness is around 9 nm (Figure 7e). These fibers are already crystalline at room temperature. They consist of small crystallites up to 50 nm in size what is seen from TEM micrograph (Figure 7b). The diffraction patterns (Figure 7c, d) show circles, where individual dots are visible and can be indexed as a mixture of cubic and hexagonal SiC (β - and α -SiC).

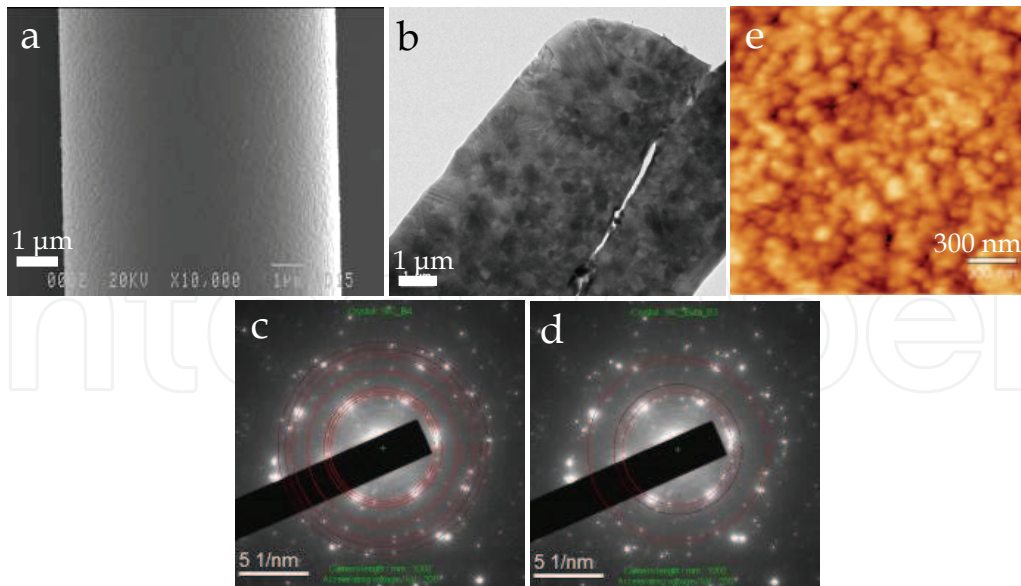


Fig. 7. Tyranno SA SiC fiber: (a) SEM micrograph; (b) TEM micrograph; (c, d) Diffraction patterns for β - and α -SiC grains; (e) AFM micrograph.

4.2 The Mechanical Properties of the SiC fibers

SiC fibers exhibit a wide distribution of diameters which was taken into account to get a reliable tensile strength data. Before measurement was done each fiber was checked with optical microscope. All the samples were glued onto paper in the shape of letter "U" to make sure, that the presence of the creep inside the clamps was eliminated. Before measuring the side section of the paper was removed using a pair of ceramic scissors. The dynamometer Instron 5567 was used, with a clamping length of 1 cm and a crosshead speed of 1 mm/min. Figure 8 shows the stress - strain curves, measured at room temperature for untreated SiC fiber (Nicalon SiC fiber @ RT) and after thermal treatment at 1300 °C for 3 h in pure argon (Nicalon SiC fiber @ 1300 °C).

Nicalon SiC fiber sample at room temperature shows, except for small deformations, mainly proportional stress dependence of the strain until the fracture at $\epsilon_p = 2,40\%$, stress $\sigma_p = 86,31 \text{ cNtex}^{-1} = 2,20 \text{ GPa}$. Stress at yield point is $\sigma_y = 7,91 \text{ cNtex}^{-1} = 0,20 \text{ GPa}$ at elastic deformation of $\epsilon_y = 0,303\%$. Elastic modulus $E = 55,20 \text{ GPa}$ is small. Work to fracture is $A_p = 4,20 \cdot 10^{-2} \text{ mJ}$ and elastic work to yield point is $A_y = 3,35 \cdot 10^{-4} \text{ mJ}$, which represents 0,80% of the total energy to break. Specific work is $A_{sp} = 1,00 \cdot 10^{-2} \text{ Jkg}^{-1}$ and a fracture work factor which represents the toughness of the material is $f_A = 0,483$.

Stress-strain curve of Nicalon SiC fiber sample after thermal treatment at 1300 °C shows different behavior. Heat treatment increases the crystallinity of SiC fiber which reflects in the strong increase of the initial elastic modulus. After the yield point, sample exhibit plastic deformation at slight increase of stress at strain of about 0,4 %. This plastic deformation is a consequence of some rearrangement of the structure which requires even higher energy at further deformation until the fracture at strain $\epsilon_p = 1,30 \%$ and fracture strength of $\sigma_p = 49,52 \text{ cNtex}^{-1} = 1,26 \text{ GPa}$. Stress at yield point is $\sigma_y = 13,25 \text{ cNtex}^{-1} = 0,33 \text{ GPa}$ at elastic strain of $\epsilon_y = 0,107 \%$. After heat treatment the elastic modulus substantially increase to $E = 328,14 \text{ GPa}$. Fracture work of heat-treated sample is due to the smaller strain smaller ($A_p = 1,34 \cdot 10^{-2} \text{ mJ}$) compared to untreated sample. Contrary, the elastic work is due

to higher stress at yield point higher ($A_y = 2,98 \cdot 10^{-4}$ mJ) and represents 2,22 % of total fracture energy. Specific work is $A_{sp} = 3,20 \cdot 10^{-3}$ Jkg⁻¹ and a fracture work factor is $f_A = 0,497$.

Parameter	Nicalon SiC fiber @ RT	Nicalon SiC fiber @ 1300 °C
Fracture strength σ_p (GPa)	2,20	1,26
Fracture strain ϵ_p (%)	2,40	1,30
Yield strength σ_y (GPa)	0,20	0,33
Yield strain ϵ_y (%)	0,303	0,107
Fracture work A_p (mJ)	$4,20 \cdot 10^{-2}$	$1,34 \cdot 10^{-2}$
Work to yield point A_y (mJ)	$3,35 \cdot 10^{-4}$	$2,98 \cdot 10^{-4}$
Specific work A_{sp} (Jkg ⁻¹)	$1,00 \cdot 10^{-2}$	$3,20 \cdot 10^{-3}$
Elastic modulus E (GPa)	55,20	328,14
Fracture-work factor f_A	0,483	0,497

Table 1. Comparison of viscoelastic parameters for untreated and thermally treated Nicalon SiC fibers.

Comparison of viscoelastic properties of both samples allows the following conclusions: After heat treatment, the elastic modulus increased by a factor 6, the material becomes more crystalline and reduces the ability of strain, as well as reduces the fracture strength. Heat-treated material has a greater capability to strain (0,4 %). In heat-treated material, the elastic deformation zone is lowered, at the same time the yield strength is higher by a factor 1,7. Yield point represents the boundary between elastic and plastic deformation. This gives the material greater stability in an otherwise narrower elastic region. Toughness of heat-treated material is reduced as can be seen from comparison of fracture work factor and specific work (energy needed to deform one kg of material).

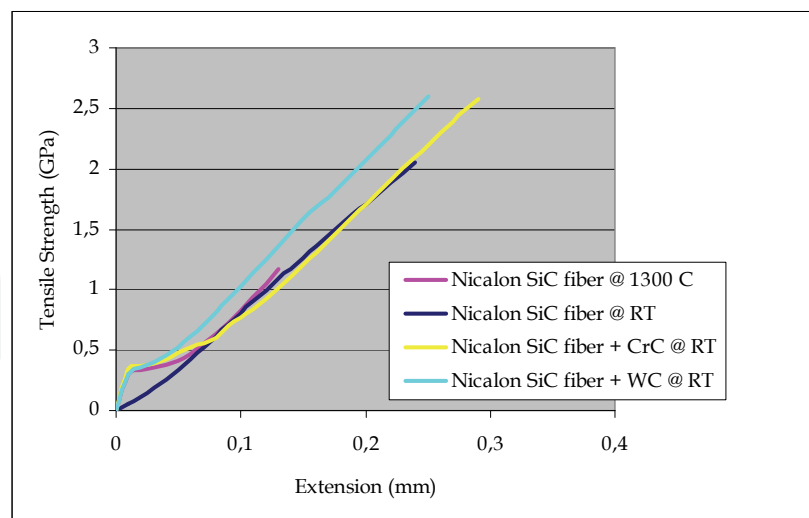


Fig. 8. Stress/strain curves for untreated and thermally treated (1300 °C for 3 h in pure argon) Nicalon SiC fibers and Nicalon SiC fibers coated with CrC and WC measured at room temperature.

In Figure 8, the stress–strain curves, measured at room temperature for Nicalon SiC fibers, coated with CrC and WC are displayed. From the curves of both samples it could be

concluded that they have approximately the same initial modulus with clearly expressed yield point at 0,12 %, the transition to plastic deformation and further hardening until fracture. High value of initial modulus is due to the presence of WC and CrC. Viscoelastic properties of both types of samples are very similar. Comparison of viscoelastic parameters for samples coated with CrC and WC is displayed in table 2.

Parameter	Nicalon SiC fiber + CrC	Nicalon SiC fiber + WC
Fracture strength σ_p (GPa)	2,77	2,78
Fracture strain ε_p (%)	2,90	2,50
Yield strength σ_y (GPa)	0,390	0,342
Yield strain ε_y (%)	0,117	0,117
Fracture work A_p (mJ)	$6,41 \cdot 10^{-2}$	$5,81 \cdot 10^{-2}$
Delo do polzišča A_y (mJ)	$3,83 \cdot 10^{-4}$	$3,39 \cdot 10^{-4}$
Specific work A_{sp} (Jkg ⁻¹)	$1,53 \cdot 10^{-2}$	$1,38 \cdot 10^{-2}$
Elastic modulus E (Gpa)	345,14	302,33
Fracture-work factor f_A	0,484	0,507

Table 2. Comparison of viscoelastic parameters for Nicalon SiC fibers coated with CrC and WC.

Parameters of viscoelastic properties of samples of Nicalon SiC fiber + CrC and Nicalon SiC fiber + WC, measured at room temperature indicate that materials have similar viscoelastic properties. Nicalon SiC fiber, coated with CrC has slightly higher initial elastic modulus and yield strength, the difference between the two types of sample is in strain between 0,5 % and fracture and consequently also higher fracture work for sample coated with CrC.

Heat treated SiC Nicalon SiC fiber sample and WC coated Nicalon SiC fiber sample have similar elastic properties up to yield point (comparable starting elastic modulus and yield strength and stress).

Tyranno SA SiC fibers are very brittle at room temperature and as such impossible to handle or measure.

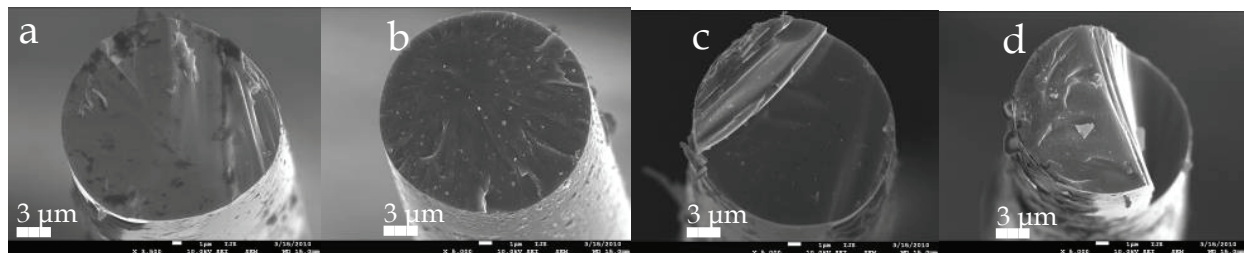


Fig. 9. SEM micrographs of the Nicalon SiC fibers fracture surfaces.

After tensile measurements all fracture surfaces of the fibers were investigated with scanning electron microscope (Figure 9a-d). In general, fracture in fibers initiates at some flaw(s), internal or on the surface. Very frequently, a near-surface flaw such as a microvoid or an inclusion is responsible for the initiation of fracture of fiber. Surface flaws are common in SiC based fibers because of the processing technique. Airborne particles as well as other elements tend to attach to the surface of the fiber during process and handling. One important feature of ceramic fiber is the surface texture. Their surface roughness scales with

gain size. The rough surface of such brittle fibers makes them break at very low strains and it makes very difficult to handle them in practice. The grain boundaries on the surface can act as notches and weaken the fiber (Elices & Llorca, 2002).

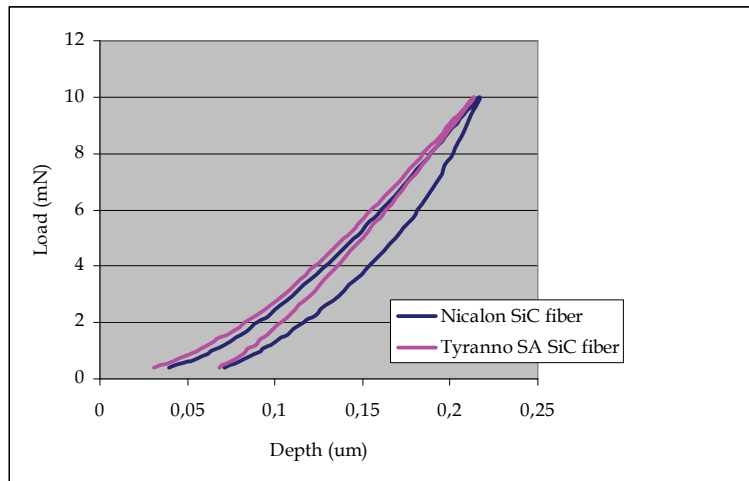


Fig. 10. Load/Depth curves for Nicalon SiC fiber and Tyranno SA SiC fiber measured at room temperature.

We also measured the nanohardness of Nicalon and Tyranno SA SiC fibers at room temperature using Vickers indenter on the Fischerscope instrument. The load we used was 10 mN. Figure 10 shows two load/depth curves, average of 10 measurements, for mentioned SiC fibers. The nanohardness for Nicalon SiC fiber is around 1800 HV and for Tyranno SA SiC fiber around 2800 HV. From the curve load/depth we can see that the elastoplastic deformation appears in both cases.

4.3 SiC Based Matrix and SiC_f/SiC composite material

In previous paragraphs the microstructure and mechanical properties of different SiC fibers were described. To produce the composite material we had to prepare a SiC matrix phase. It was made from water suspension of SiC particles and sintering additive based on low-melting-point eutectic composition of the Al-Si-P-O system, which enables sintering at low temperature and thus avoids the change in the microstructure of the SiC fibers. Figure 11a shows SEM micrograph of the matrix, from where we can see that the size of the particles is less than 1 μm . Figures 11b, c show cross-sectional SEM micrographs at different magnifications of the composite material with Nicalon SiC fibers produced with a method described above. Large pores observed in all the samples were made during the mechanical grinding and polishing as part of the sample preparation. The matrix was fully filled up the areas around the fiber bundle. The effectiveness of the adhesion between the fibers and the matrix was checked on thermally treated samples using TEM and microanalysis (Figures 11d, e). Nicalon SiC fibers have a 50 nm thick SiO₂ amorphous layer on the surface after thermal treatment (Figure 11e).

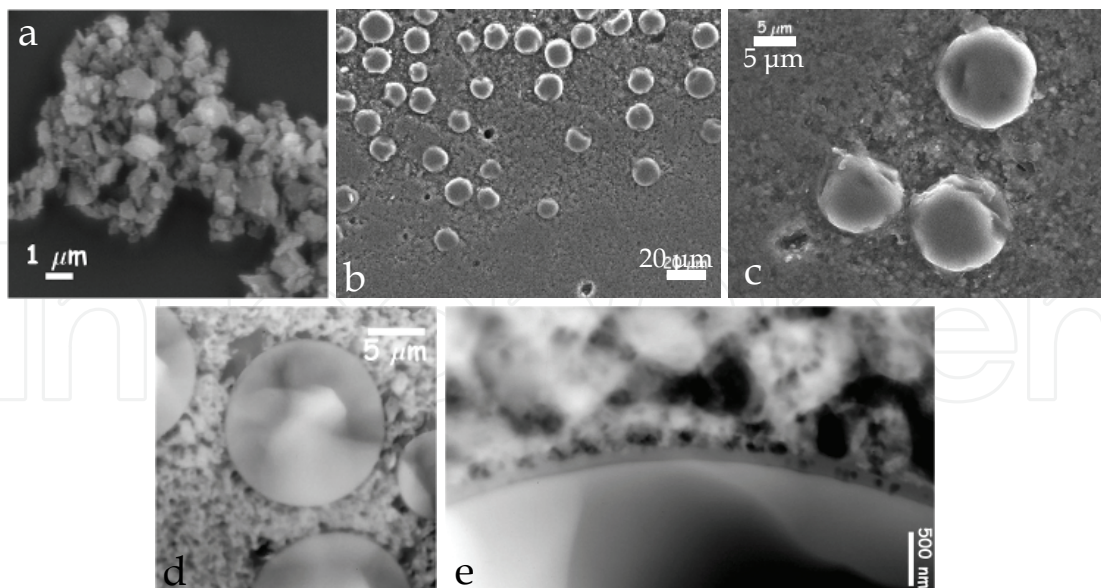


Fig. 11. SEM and TEM micrographs of SiC matrix and SiC_f/SiC composite material: (a) SiC matrix; (b) SiC_f/SiC composite material; (c) The same as (b) but at higher magnification; (d) SiC_f/SiC prepared by tripod polishing; (e) Reaction layer on the fiber surface.

4.4 Interphases in SiC_f/SiC composite material

According to the literature (Xin-Bo & Hui, 2005; Xin-Bo et al., 2000; Bertrand et al., 2001; Nuriel et al., 2005) the role of the interphase is very important. It determines the mechanical and physical properties of ceramic matrix composites (CMCs). Although the SiC_f/SiC composite material has many advantages, it also has one important disadvantage; the brittleness. Figure 12a shows SEM micrograph of the SiC_f/SiC composite material, where the crack path introduced by the Vickers indenter continued through the fibers. This would lead to a catastrophic failure of the composite material.

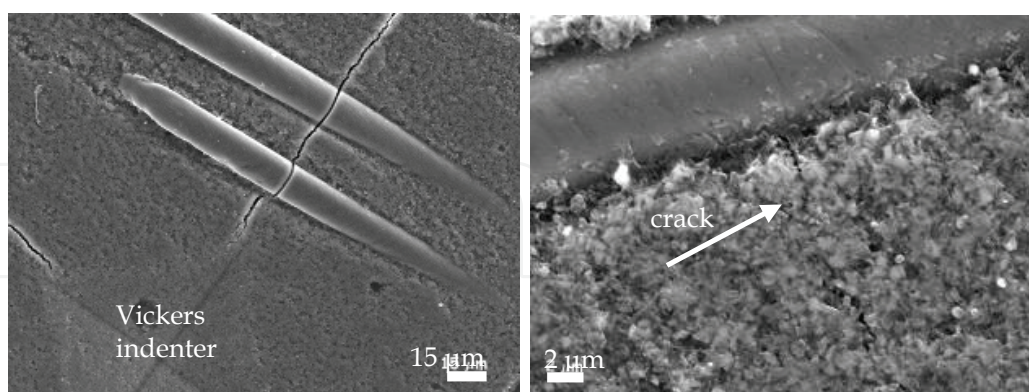


Fig. 12. SEM micrographs of (a) a failure of the composite material and (b) the crack deflection on the fiber/matrix interface (500 nm thick CrN was used as an interphase).

A crack deflection mechanism requires a weak fiber/matrix bond so that as a matrix crack reaches the interface, it gets deflected along the interface rather than passing straight through the fiber. A weak interfacial bond also leads to fiber pullout.

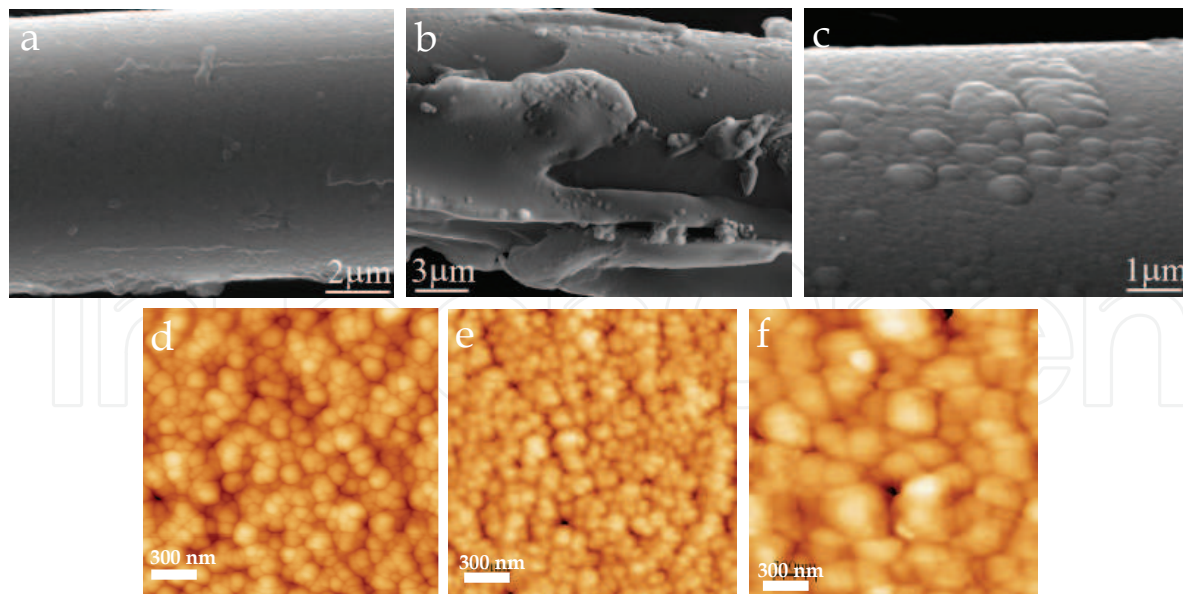


Fig. 13. SEM and AFM micrographs of Nicalon SiC and Tyranno SA SiC fibers: (a, d) Tyranno SA SiC fiber coated with DLC; (b, e) Nicalon SiC fiber coated with WC; (c, f) Nicalon SiC fiber coated with CrC.

In order to prevent a catastrophic failure of the composite material under load, various thin layers have been deposited on the surface of the fibers by physical vapor deposition, using reactive sputtering. The layers were selected on the basis of the relevant chemical composition appropriate for use in a future fusion reactor. Figure 13 shows SEM micrographs of three interface materials; DLC (diamond-like carbon), WC and CrC. All three layers were deposited along the fiber axis with the thickness varying between a few nm and 0.5 μm , depending on the geometry and conditions during the deposition. From AFM micrographs we can see the difference in roughness before and after the deposition. DLC layer was deposited on Tyranno SA SiC fiber. The roughness is almost the same, around 9 nm. WC and CrC were deposited on Nicalon SiC fibers from where we can see that the difference in roughness is quite big. In the case of WC, the roughness changes from 2 to 7 nm and in the case of CrC from 2 to 15 nm.

We also used CrN, but according to the literature (Taguchi et al., 2005) this kind of interface is not suitable for fusion applications because the nitrogen transmutes into ^{14}C , which has a very long half-life as a β emitter after the neutron irradiation. We also encountered another problem, a reaction between the thin layer (CrN) and the matrix. TEM analysis showed that after sintering the CrN partially diffused into the matrix around the fibers. Nevertheless, the CrN layer caused a deflection of the crack from its primary direction and thus prevents the fiber from cracking (Figure 12b).

In the case of WC coating, a multilayer (sandwich structure) approach was used in order to improve the mechanical properties. Figure 14a shows TEM micrograph of the WC coating on the surface of the Nicalon SiC fiber. The WC was deposited as a sandwich structure. The first layer, with a thickness of 40 nm, is crystalline chromium, which ensures better cling of WC to the fiber surface. The second layer, with a thickness of 18 nm, is pure tungsten which enables a more continuous transition of WC. These layers also ensured better adhesion of

the coating to the fiber surface. The third layer is amorphous tungsten carbide, with a thickness of 400–500 nm.

Similar approach was also used in the case of CrC. The first layer, with a thickness up to 80 nm was nanocrystalline chromium, which ensures better cling of CrC to the fiber surface. The second layer was chromium carbide, with a thickness of 400–500 nm (Figure 14b). The problem that was observed was a columnar growth of CrC. The crack that would initiate in the matrix phase would not stop at the CrC/matrix interface but because of the columnar growth it could continue between columns until it would reach the CrC/Cr interface.

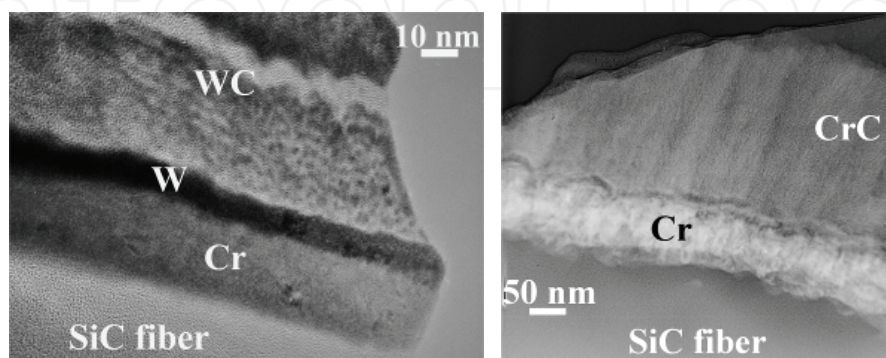


Fig. 14. TEM micrograph of sandwich structure of Nicalon SiC fibers coated with (a) WC and (b) CrC.

5. Conclusion

Different TEM specimen preparation techniques for uncoated and coated SiC fibers, ceramic material and ceramic composite material were described, all with their advantages and disadvantages. The conventional technique which is made up from mechanical thinning, dimpling and ion-milling is not suitable for observing the SiC fibers because the fibers are much stiffer than the epoxy in which the fibers are embedded during the preparation. Although the method that combines a technique for preparing fiber/epoxy assemblies with mechanical polishing to a thickness of less than 5 μm , thus minimizing the time of ion milling, requires a long preparation time, frequently observations under optical microscope to ensure parallel thinning and accuracy it is suitable for SiC fibers.

The microstructure of SiC fibers was observed using scanning and transmission electron microscope and atomic force microscope.

Using dynamometer Instron 5567 the tensile properties were measured. If we compare untreated and thermally treated Nicalon SiC fibers we can see, that the elastic modulus is increased by a factor 6, the material becomes more crystalline and reduces the ability of strain, as well as reduces the fracture strength. Nicalon SiC fibers, coated with CrC and WC, have similar viscoelastic properties which are similar to thermally treated Nicalon SiC fibers up to yield point (comparable starting elastic modulus and yield strength).

The nano-hardness of the matrix is 300 HV, which is 6 times lower than for Nicalon SiC fibers and 9 times lower than for Tyranno SA SiC fibers.

A novel method for preparing SiC_f/SiC composite material for a future fusion reactor has been shown to be quite promising. The sintering additive used in the matrix was based on a low-melting-point eutectic composition in the Al-Si-P-O system, which enables sintering at low temperatures, in order to avoid the recrystallization of the Nicalon SiC-fibers and thus avoid embrittlement of the fibers and degradation of the mechanical properties.

Uncoated SiC-fibers have, after thermal treatment, a 50-nm-thick SiO₂ amorphous layer on the surface, which does not prevent the cracks from propagating at the fiber/matrix interface. This leads to a catastrophic failure of the composites. To control the matrix-to-fiber stress transfer (crack deflection at the fiber/matrix interface) Nicalon and Tyranno SiC-fibers were coated with various thin layers of different chemical compositions, such as CrC, WC and DLC, by physical vapor deposition, leading to composites with different degrees of toughness. Of the deposited layers that deflect cracks, CrN is not useful because nitrogen transmutes into ¹⁴C and the CrN diffused into the matrix around the fibers.

6. Acknowledgements

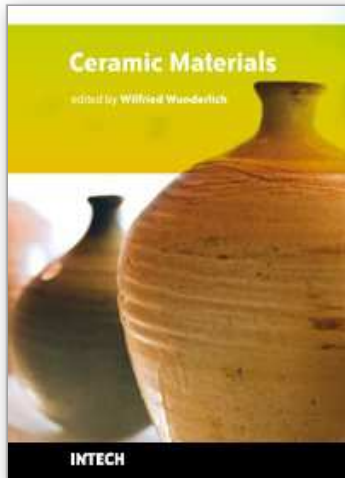
Mrs. Medeja Gec is acknowledged for her help in TEM sample preparation and Mr. Matjaz Panjan and Dr. Peter Panjan from the Department of Thin films and Surfaces, Jozef Stefan Institute, Slovenia, are thanked for their help in depositing the thin films on the fiber surface and the Vickers indent experiments. This work was performed under the contract P2-0084 and was financially supported by the Ministry of Higher Education, Science and Technology of the Republic of Slovenia and the European Commission within the Contract of Association Euratom FU06-CT-2004-00083.

7. References

- Bertrand, S.; Droillard, C.; Pailler, R.; Bourrat, X. & Naslain, R. (2000). TEM structure of (PyC/SiC)_n multilayered interphases in SiC/SiC composites. *Journal of the European Ceramic Society*, Vol. 20, No. 1, (January 2000) 1-13
- Bertrand, S.; Pailler, R. & Lamon, J. (2001). SiC/SiC minicomposites with nanoscale multilayered fibre coatings. *Composites Science and Technology*, Vol. 61, No. 3, (February 2001) 363-367
- Chawla, K. K. (1987). *Composite Materials: Science and Engineering*, Springer-Verlag, ISBN 0-387-96478-9, New York
- Drazic, G.; Novak, S.; Daneu, N. & Mejak, K. (2005). Preparation and Analytical Electron Microscopy of a SiC Continuous-Fiber Ceramic Composite. *Journal of Materials Engineering and Performance*, Vol. 14, No. 4, (August 2005) 424-429, ISSN 1059-9495
- Elices, M. & Llorca, J. (2002). *Fiber Fracture*, Elsevier Science, ISBN-13 : 978-0-08-044104-7, Kidlington, Oxford
- Gec, M. & Ceh, M. (2006). Tehnike priprave vzorcev za preiskave na TEM (1. del) - Mehanska predpriprava vzorca. *Vakuumist*, Vol. 26, No. 1-2, (June 2006) 23-29, ISSN 0351-9716
- Jacques, S.; Lopez-Marure, A.; Vincent, C.; Vincent, H. & Bouix, J. (2000). SiC/SiC minicomposites with structure-graded BN interphases. *Journal of the European Ceramic Society*, Vol. 20, No. 12, (November 2000) 1929-1938
- Katoh, Y.; Dong, S. M. & Kohyama, A. (2002). Thermo-mechanical properties and microstructure of silicon carbide composites fabricated by nano-infiltrated transient eutectoid process. *Fusion Engineering and Design*, Vol. 61-62, (November 2002) 723-731
- Kowbel, W.; Withers, J. C.; Loutfy, R. O.; Bruce, C. & Kyriacou, C. (1995). Silicon carbide fibers and composites from graphite precursors for fusion energy applications. *Journal of Nuclear Materials*, Vol. 219, (1995) 15-25, ISSN 0022-3115
- Mogilevsky, P. (2002). Preparation of thin ceramic monofilaments for characterization by TEM. *Ultramicroscopy*, Vol. 92, No. 3-4, (August 2002) 159-164

- Novak, S.; Koenig, K. & Drazic, G. (2006). The preparation of LPS SiC-fibre-reinforced SiC ceramics using electrophoretic deposition. *Journal of Material Science*, Vol. 41, No. 24, (October 2006) 8093-8100
- Novak, S.; Drazic, G.; Koenig, K. & Ivekovic, A. (2010). Preparation of SiCf/SiC composites by the slip infiltration and transient eutectoid (SITE) process. *Journal of Nuclear Materials*, Vol. 399, No. 2-3, (2010) 167- 174
- Nuriel, S.; Liu, L.; Barber, A. H. & Wagner, H. D. (2005). Direct measurement of multiwall nanotube surface tension. *Chemical Physics Letter*, Vol. 404, No. 4-6, (March 2005) 263-266
- She, J. H. & Ueno, K. (1999). Effect of additive content on liquid-phase sintering on silicon carbide ceramics. *Materials Research Bulletin*, Vol. 34, (1999) 1629-1636
- Stadelman, P. A. (1987). EMS - a software package for electron diffraction analysis and HREM image simulation in materials science. *Ultramicroscopy*, Vol. 21, No. 2, (1987) 131
- Taguchi, T.; Igawa, N.; Yamada, R. & Jitsukawa, S. (2005). Effect of thick SiC interphase layers on microstructure, mechanical and thermal properties of reaction-bonded SiC/SiC composites. *Journal of Physics and Chemistry of Solids*, Vol. 66, No. 2-4, (February-April 2005) 576-580
- Xin-Bo, H. & Hui, Y. (2005). Preparation of SiC fiber-reinforced SiC composites. *Journal of Materials Processing Technology*, Vol. 159, No. 1, (January 2005) 135-138
- Xin-Bo, H.; Xin-Ming, Z.; Chang-Rui, Z.; Xin-Gui, Z. & An-Chen, Z. (2000). Microstructures and mechanical properties of Cf/SiC composites by precursor pyrolysis-hot pressing. *Materials Science and Engineering A*, Vol. 284, No. 1-2, (May 2000) 211-218
- Zhang, W.; Hinoki, T.; Katoh, Y.; Kohyama, A.; Noda, T.; Muroga, T. & Yu, J. (1998). Crack initiation and growth characteristics in SiC/SiC under indentation test. *Journal of Nuclear Materials*, Vol. 258-263, No. 2, (October 1998) 1577-1581

IntechOpen



Ceramic Materials

Edited by Wilfried Wunderlich

ISBN 978-953-307-145-9

Hard cover, 228 pages

Publisher Sciyo

Published online 28, September, 2010

Published in print edition September, 2010

This is the first book of a series of forthcoming publications on this field by this publisher. The reader can enjoy both a classical printed version on demand for a small charge, as well as the online version free for download. Your citation decides about the acceptance, distribution, and impact of this piece of knowledge. Please enjoy reading and may this book help promote the progress in ceramic development for better life on earth.

How to reference

In order to correctly reference this scholarly work, feel free to copy and paste the following:

Tea Toplisek, Goran Drazic, Vilibald Bukosek, Sasa Novak and Spomenka Kobe (2010). Electron Microscopy and Microanalysis of the Fiber, Matrix and Fiber/Matrix Interface in SiC Based Ceramic Composite Material for Use in a Fusion Reactor Application, Ceramic Materials, Wilfried Wunderlich (Ed.), ISBN: 978-953-307-145-9, InTech, Available from: <http://www.intechopen.com/books/ceramic-materials/electron-microscopy-and-microanalysis-of-the-fiber-matrix-and-fiber-matrix-interface-in-sic-based-ce>

INTECH
open science | open minds

InTech Europe

University Campus STeP Ri
Slavka Krautzeka 83/A
51000 Rijeka, Croatia
Phone: +385 (51) 770 447
Fax: +385 (51) 686 166
www.intechopen.com

InTech China

Unit 405, Office Block, Hotel Equatorial Shanghai
No.65, Yan An Road (West), Shanghai, 200040, China
中国上海市延安西路65号上海国际贵都大饭店办公楼405单元
Phone: +86-21-62489820
Fax: +86-21-62489821

© 2010 The Author(s). Licensee IntechOpen. This chapter is distributed under the terms of the [Creative Commons Attribution-NonCommercial-ShareAlike-3.0 License](#), which permits use, distribution and reproduction for non-commercial purposes, provided the original is properly cited and derivative works building on this content are distributed under the same license.

IntechOpen

IntechOpen